

Supplementary Figures

Figure S1

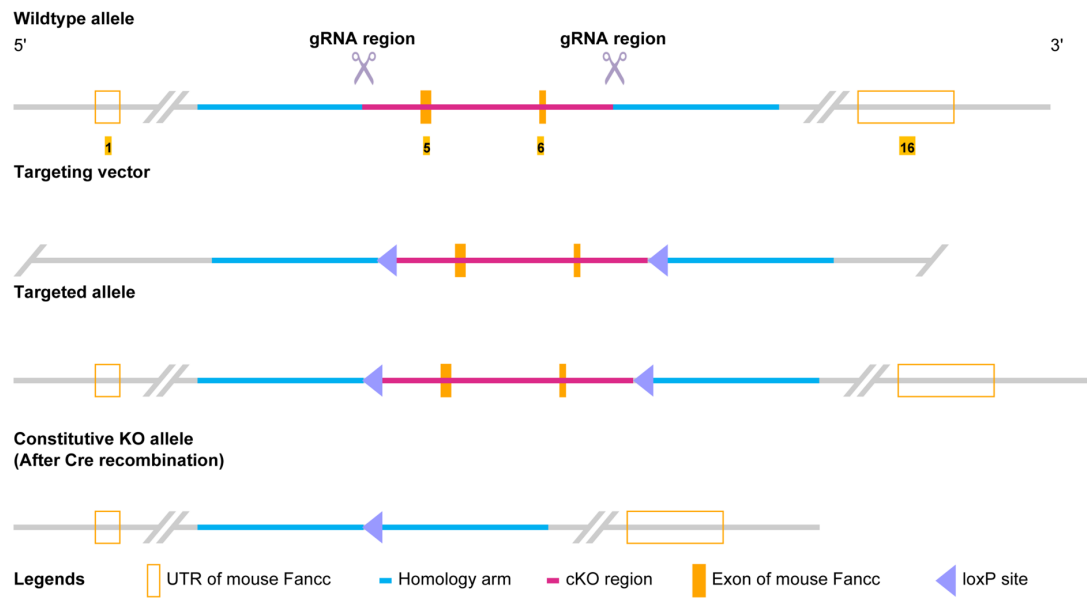


Figure S1

Targeting strategy for the FANCC cKO mice.

Figure S2

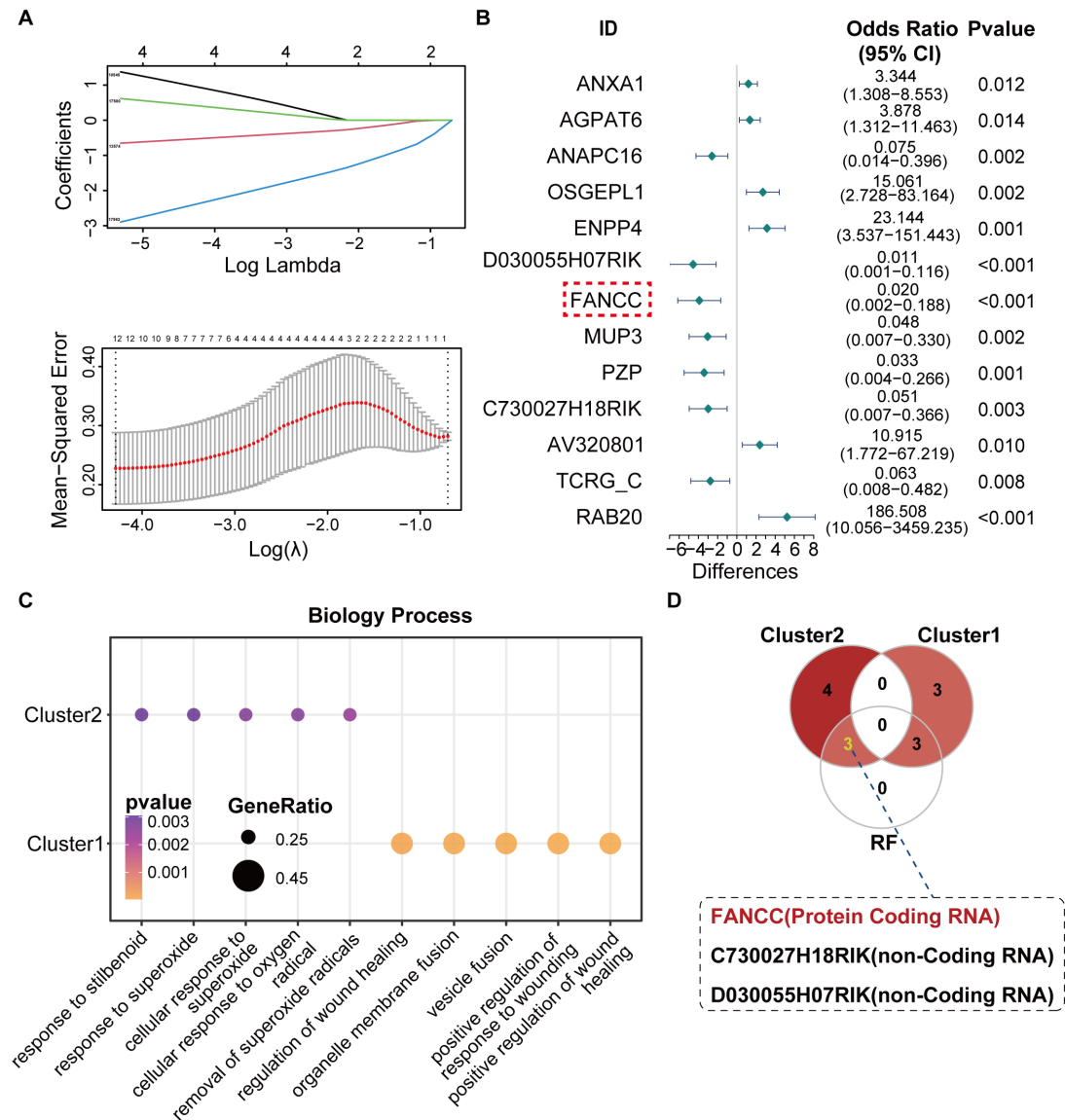


Figure S2

(A) LASSO regression penalized dimension reduction analysis to identify genes closely associated with SCI. (B) Logistic regression risk model identified 13 genes associated with SCI. (C) Enrichment analysis of genes in Clusters 1 and 2. (D) Co-expression analysis between Clusters 1 and 2, according to a random forest model.

Figure S3

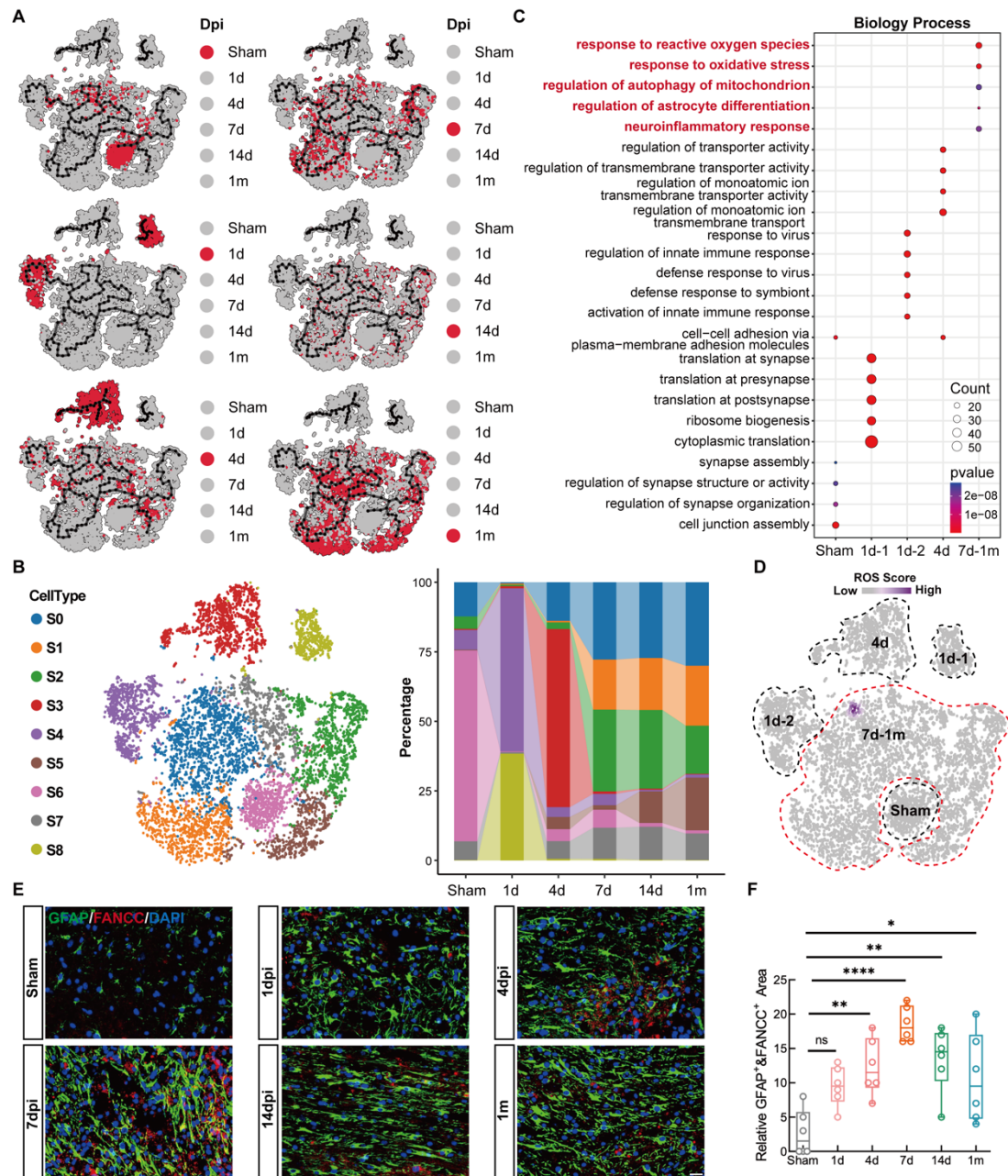


Figure S3

(A) Differentiation trajectories of astrocytes identified at different time points. Red indicates cells detected at each respective time point. (B) Proportions of each astrocyte subtype at different time points. (C) Bubble plot of the top five biological processes associated with different astrocyte states. The x-axis represents astrocyte states, the y-axis represents GO terms, dot size indicates the number of genes, and dot color

represents the p-value. **(D)** Expression of the ROS Score across five astrocyte states, calculated using a weighted kernel density algorithm. Purple represents the density intensity of the ROS Score. **(E)** Fluorescent expression changes of FANCC in astrocytes of spinal cord within 1m after injury; scale bar = 20 μ m. **(F)** Quantitative analysis of FANCC-positive and GFAP-positive area within 1m after injury. Data are presented as mean \pm SD. Statistical significance was defined as *p < 0.05, **p < 0.01, ***p < 0.001, ****p < 0.0001, and no significance (n.s.).

Figure S4

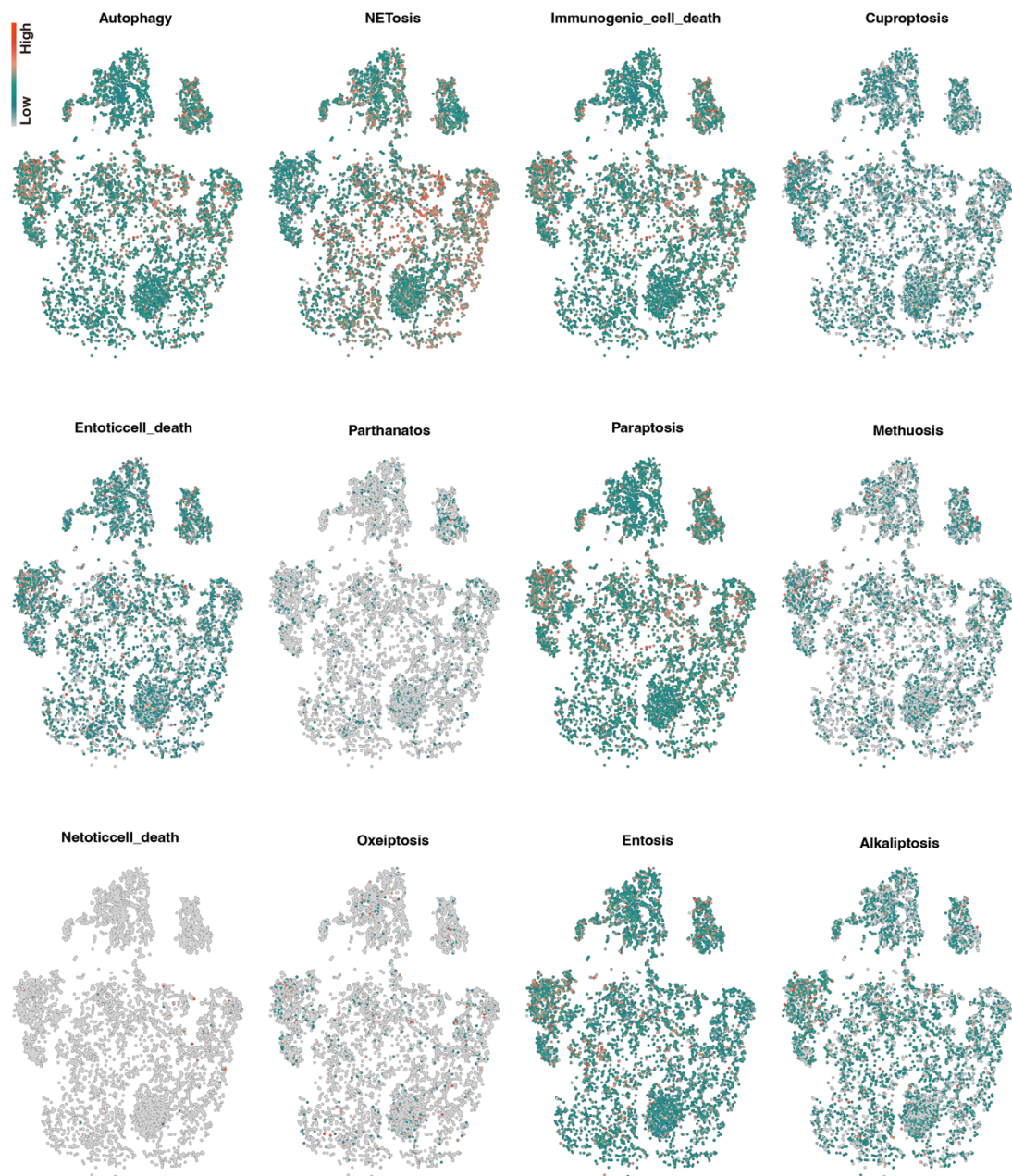


Figure S4

Scores of 12 cell death phenotypes calculated using the weighted nuclear density algorithm.

Figure S5

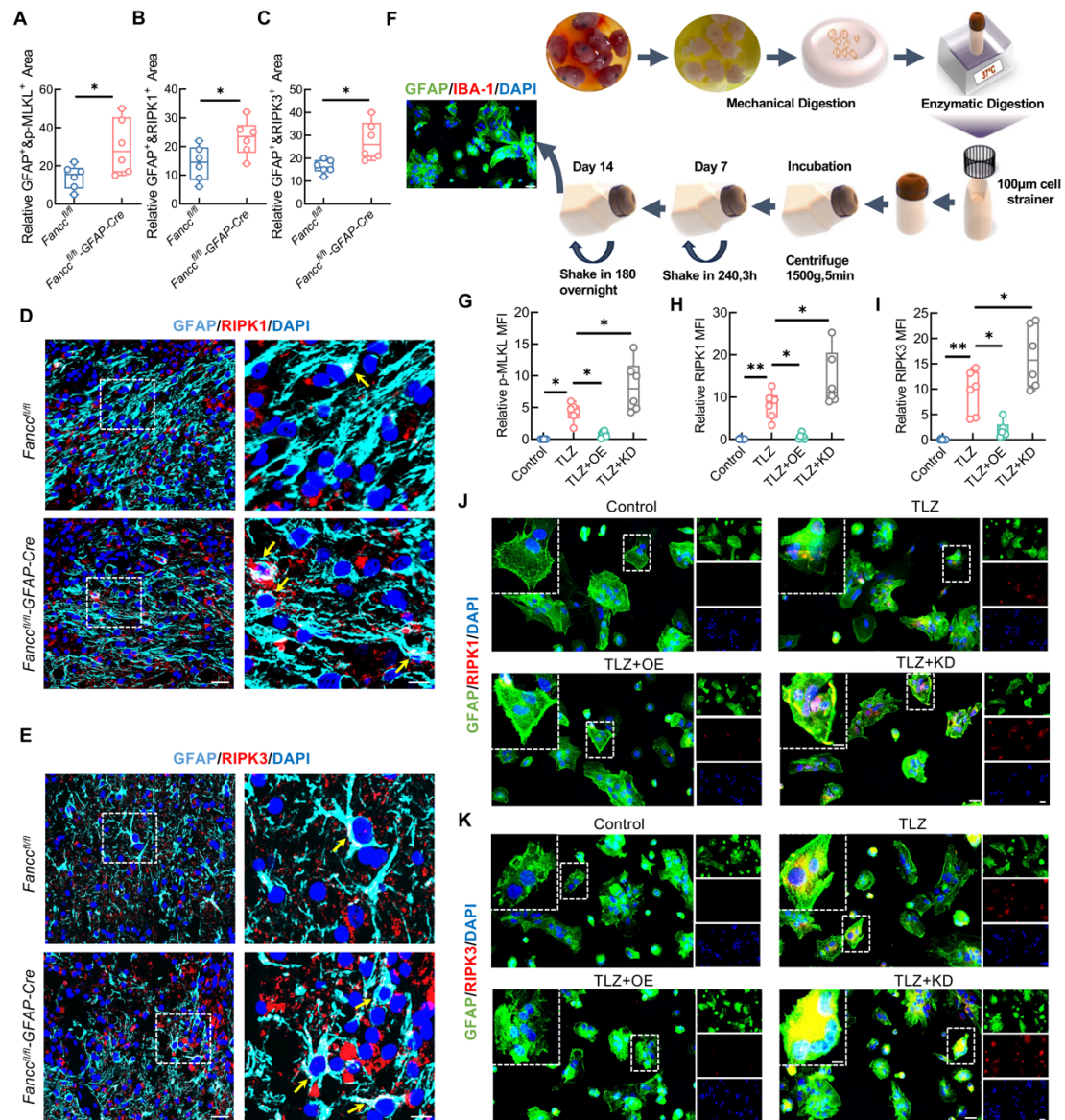


Figure S5

(A) Quantitative analysis of p-MLKL-positive and GFAP-positive area in *Fance*^{fl/fl} and *Fance*^{fl/fl}-GFAP-Cre mice at 7 dpi. (B) Quantitative analysis of RIPK1-positive and GFAP-positive area in *Fance*^{fl/fl} and *Fance*^{fl/fl}-GFAP-Cre mice at 7 dpi. (C) Quantitative analysis of RIPK3-positive and GFAP-positive area in *Fance*^{fl/fl} and *Fance*^{fl/fl}-GFAP-Cre mice at 7 dpi. (D) Representative IF images of RIPK1 (red) and GFAP (green) in the spinal cord in *Fance*^{fl/fl} and *Fance*^{fl/fl}-GFAP-Cre mice at 7 dpi; scale bar = 25/10 µm. (E) Representative IF images of RIPK3 (red) and GFAP (green) in the spinal cord in

Fance^{fl/fl} and *Fance*^{fl/fl}-*GFAP-Cre* mice at 7 dpi; scale bar = 25/10 μm . (F) Schematic diagram of the extraction process of primary astrocytes. (G-I) Quantitative analysis of p-MLKL, RIPK1 and RIPK3 fluorescence expression in astrocytes treated with TLZ for 48 h after transfection with FANCC-OE or FANCC-KD. (J) Representative IF images of RIPK1 (red) and GFAP (green) in astrocytes treated with TLZ for 48 h after transfection with FANCC-OE or FANCC-KD; scale bar = 50/20/50 μm . (K) Representative IF images of RIPK3 (red) and GFAP (green) in astrocytes treated with TLZ for 48 h after transfection with FANCC-OE or FANCC-KD; scale bar = 50/20/50 μm . Data are presented as mean \pm SD. Statistical significance was defined as * $p < 0.05$, ** $p < 0.01$, *** $p < 0.001$, **** $p < 0.0001$, and no significance (n.s.).

Figure S6

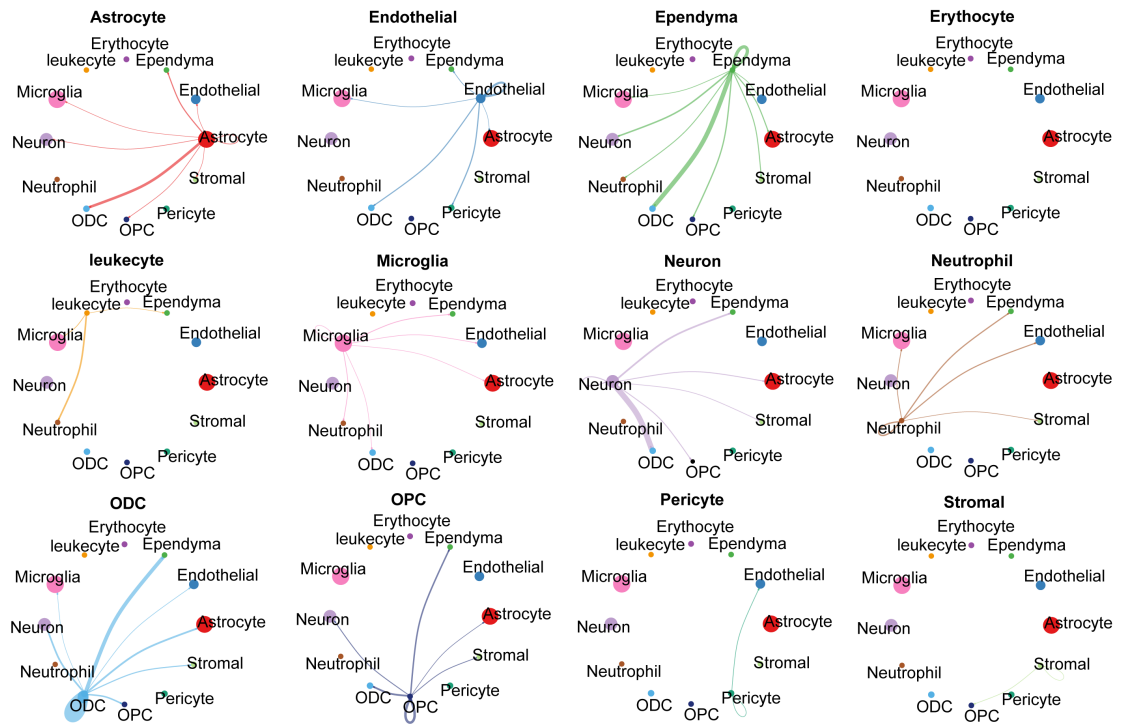


Figure S6

Interactions between different cell types in the spinal cord after SCI.

Figure S7

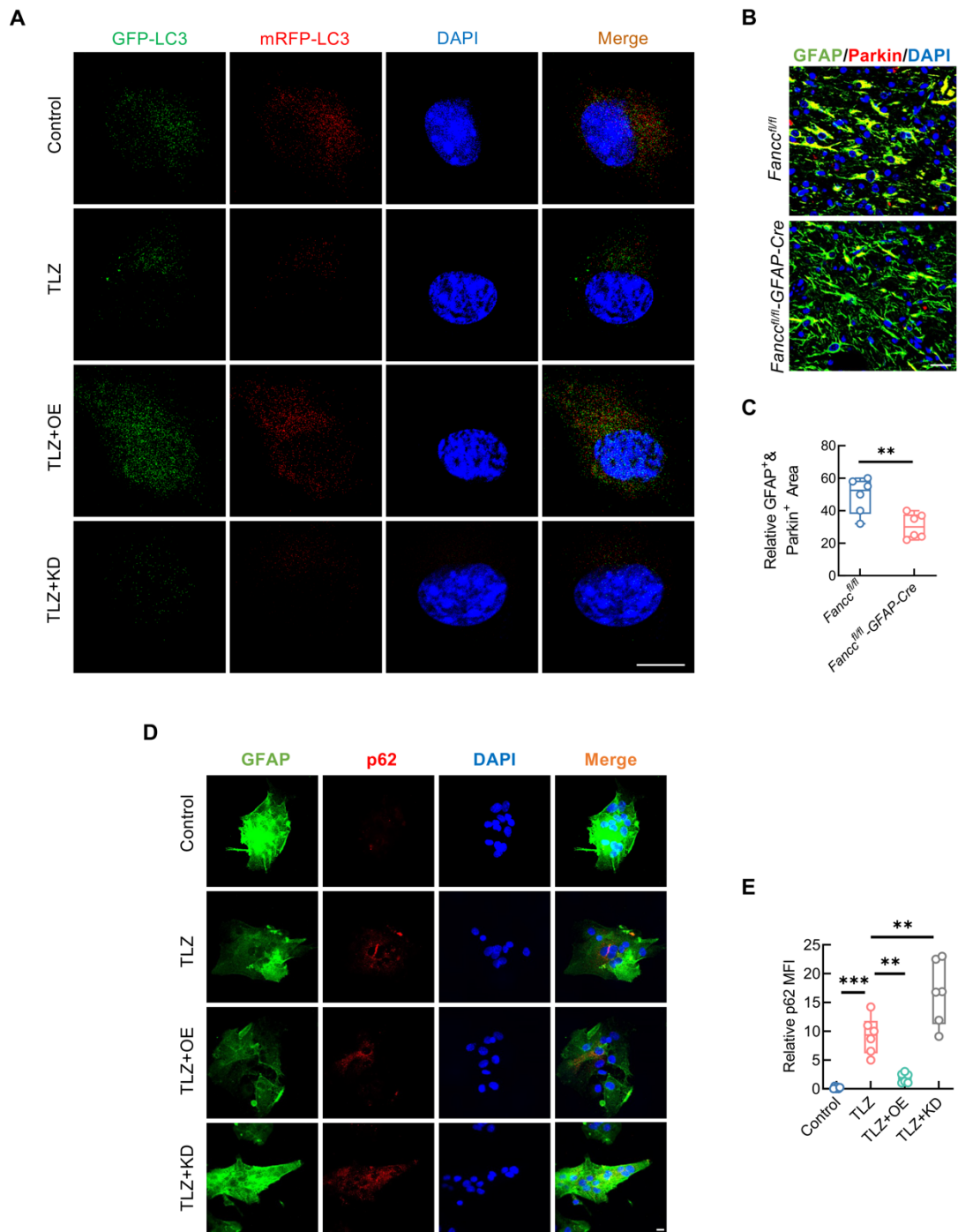


Figure S7

(A) Fluorescent localization of autophagosomes (yellow) and autolysosomes (red) using the GFP-mRFP-LC3 probe; scale bar = 10 μ m. (B) Representative IF images of Parkin (red) and GFAP (green) in the spinal cord in *Fance^{fl/fl}* and *Fance^{fl/fl}-GFAP-Cre* mice at 7 dpi; scale bar = 20 μ m. (C) Quantitative analysis of Parkin-positive and

GFAP-positive area in *Fance^{f/f}* and *Fance^{f/f}-GFAP-Cre* mice at 7 dpi. **(D)** Representative IF images of p62 (red) and GFAP (green) in astrocytes treated with TLZ for 48 h after transfection with FANCC-OE or FANCC-KD; scale bar = 20 μ m. **(E)** Quantitative analysis of p62 fluorescence expression in astrocytes treated with TLZ for 48 h after transfection with FANCC-OE or FANCC-KD. Data are presented as mean \pm SD. Statistical significance was defined as *p < 0.05, **p < 0.01, ***p < 0.001, ****p < 0.0001, and no significance (n.s.).

Figure S8

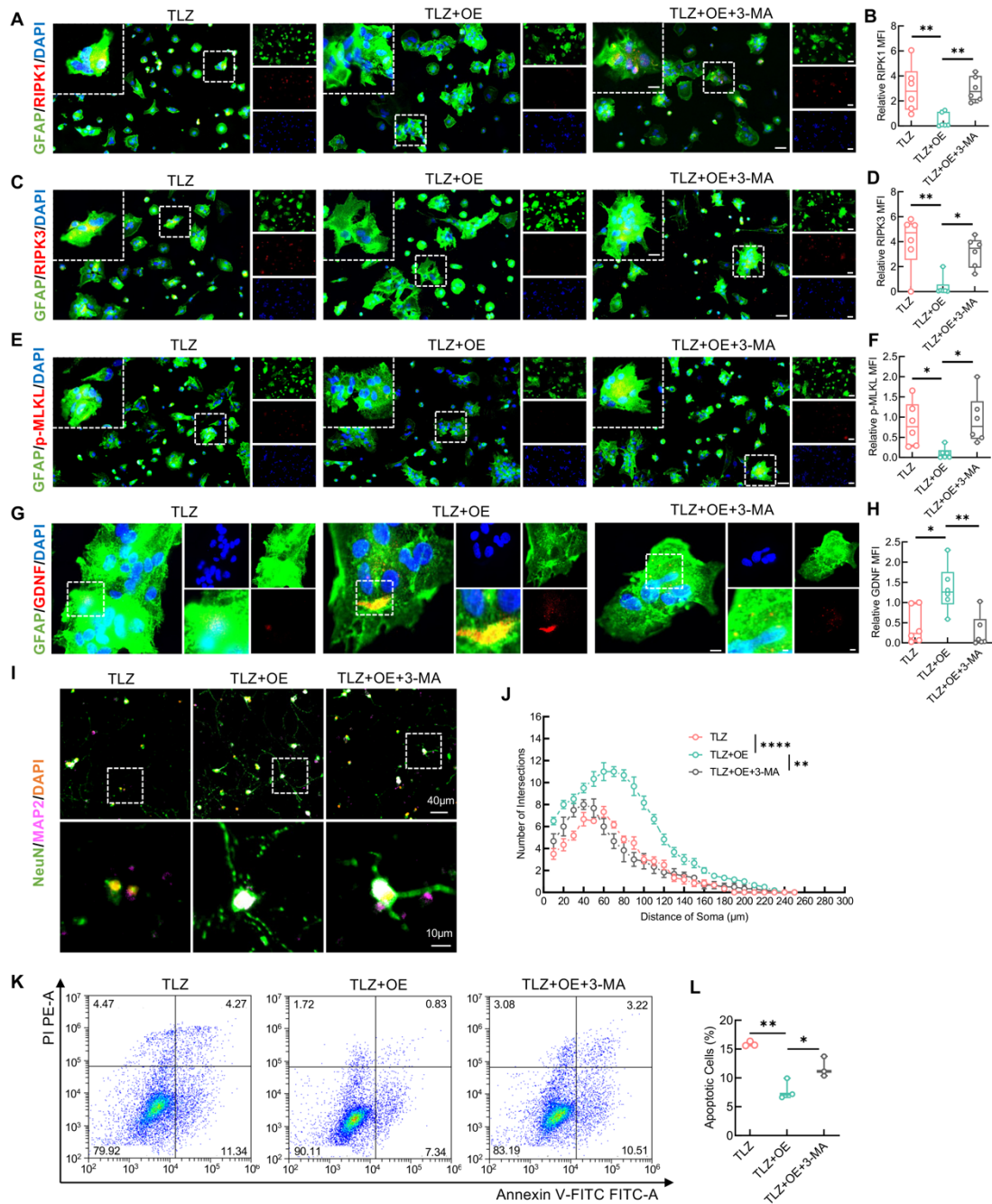


Figure S8

(A, C, E, G) Representative IF images of GFAP (green) and RIPK1, RIPK3, p-MLKL and GDNF (red) in astrocytes treated with TLZ and 5 mM 3-MA after transfection with FANCC-OE; scale bar = 50/20/50 μ m. (B, D, F, H) Quantitative analysis of RIPK1, RIPK3, p-MLKL and GDNF fluorescence expression in astrocytes treated with TLZ

and 5 mM 3-MA after transfection with FANCC-OE. **(I)** Representative IF images of NeuN (green) and MAP-2 (pink) in neurons; scale bar = 40/10 μ m. **(J)** Quantification of intersections by Sholl analysis. **(K)** Representative images of FCM results with labeling of PI and annexin-V-FITC in neurons. **(L)** Percentage of apoptotic neurons. Data are presented as mean \pm SD. Statistical significance was defined as * $p < 0.05$, ** $p < 0.01$, *** $p < 0.001$, **** $p < 0.0001$, and no significance (n.s.).

Figure S9

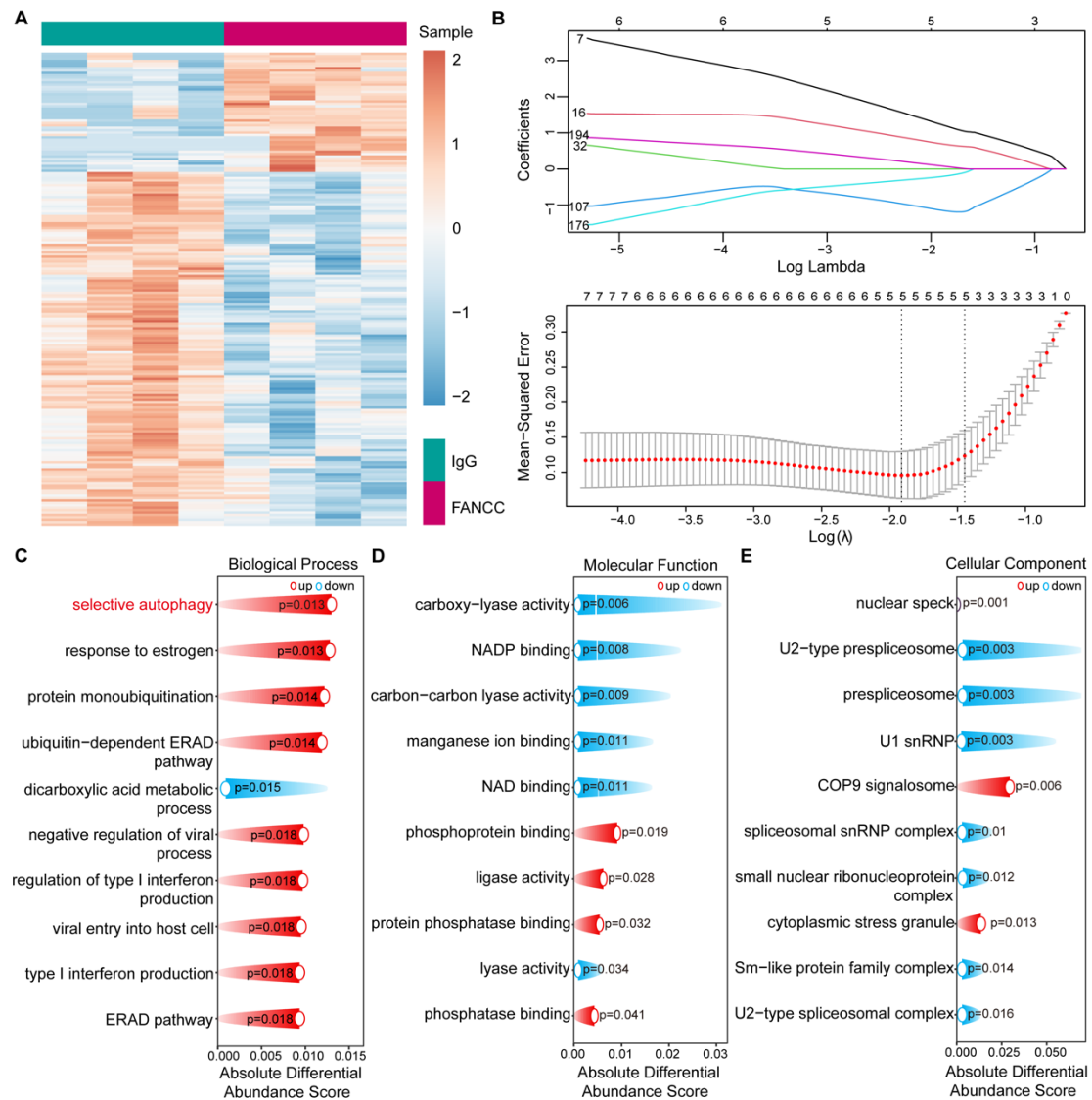


Figure S9

(A) Heatmap of differential protein analysis from 5D proteomics after Co-IP. (B) LASSO regression penalized dimension reduction analysis to identify downstream proteins with a higher association with FANCC. (C-E) Functional enrichment analysis of the selected proteins. Biological processes were mainly enriched in selective autophagy.

Figure S10

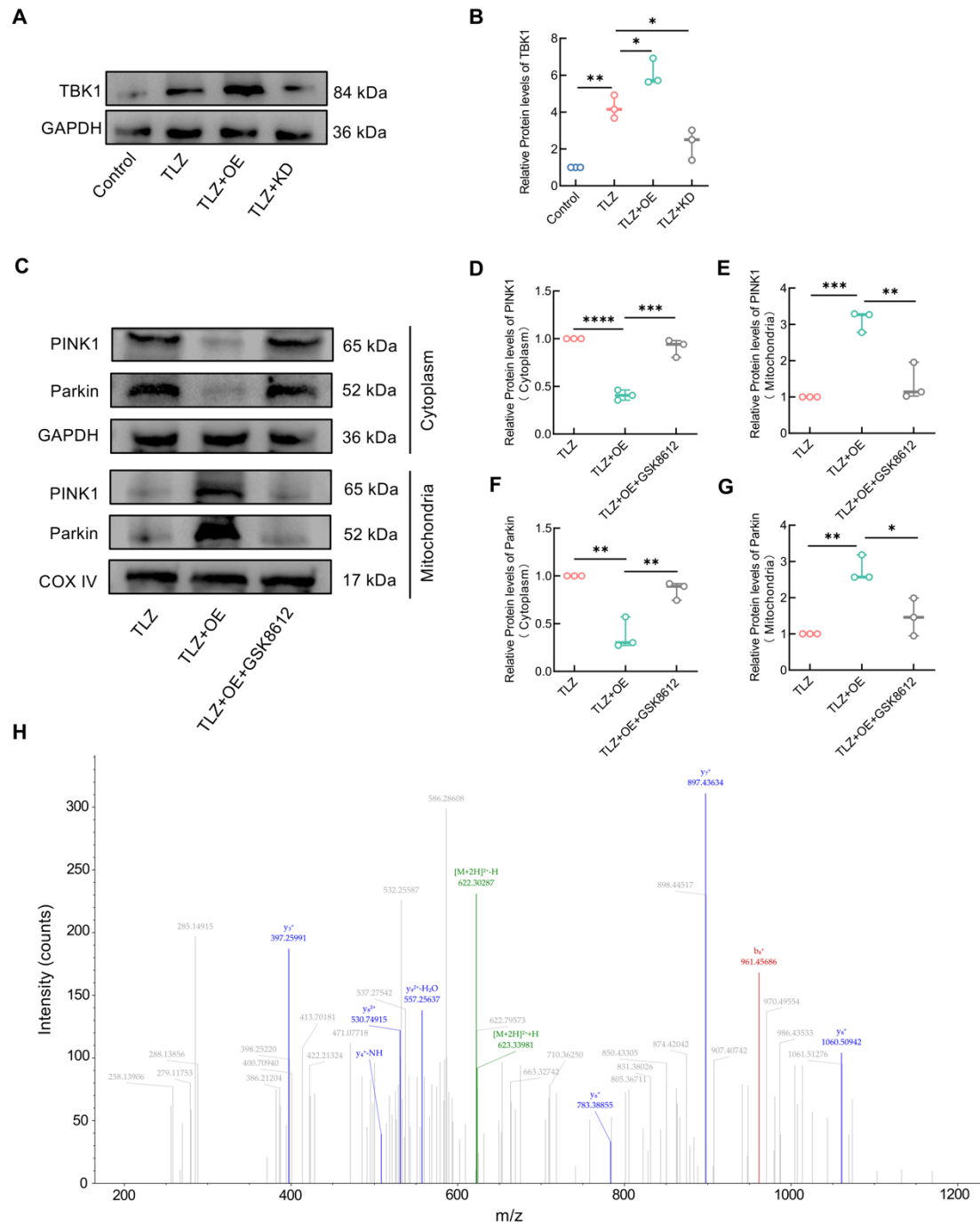


Figure S10

(A) Western blotting of TBK1 expression in astrocytes treated with TLZ for 48 h after transfection with FANCC-OE or FANCC-KD. (B) Densitometric analysis of TBK1 expression. (C) Western blotting of PINK1 and Parkin expression in cytoplasm or mitochondria of astrocytes treated with TLZ and 5 μM GSK8612 after transfection with

FANCC-OE. **(D-G)** Densitometric analysis of PINK1 and Parkin expression in cytoplasm or mitochondria. **(H)** MS analysis showed the secondary peak diagram of the TBK1 575-584 peptide. Data are presented as mean \pm SD. Statistical significance was defined as * $p < 0.05$, ** $p < 0.01$, *** $p < 0.001$, **** $p < 0.0001$, and no significance (n.s.).

Figure S11

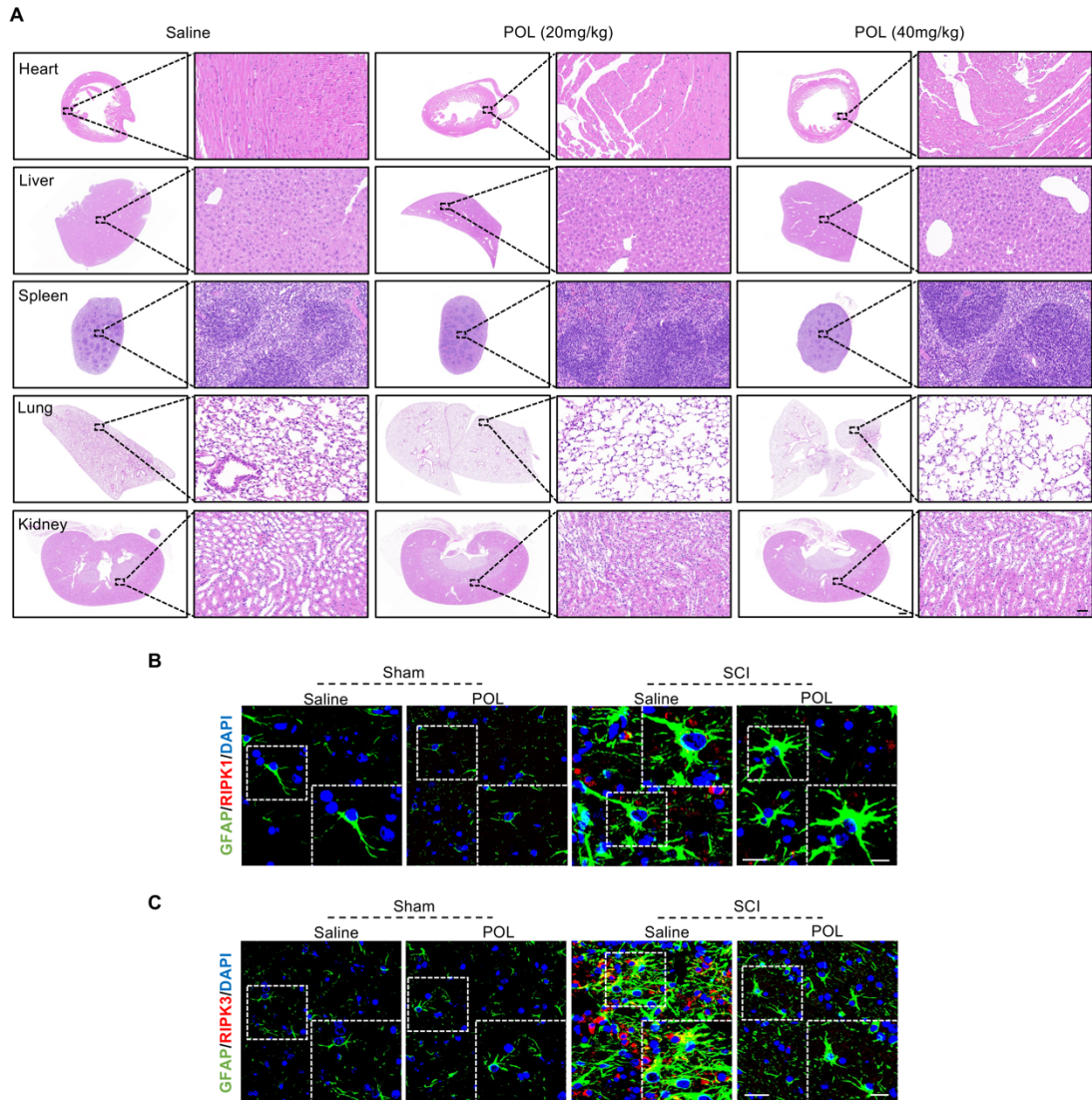


Figure S11

(A) HE staining revealed no apparent damage in the mouse heart, liver, spleen, lungs and kidneys following treatment with low and high doses of poliumoside; scale bar = 500/40 μm . (B-C) Representative IF images of RIPK1 or RIPK3 (red) and GFAP (green) in the spinal cord after treatment with poliumoside; scale bar = 20/10 μm .